Comparison of 3D finite-element and finite-difference inversion of magnetotelluric data in Okuaizu geothermal area, northern Japan

Toshihiro Uchida[1] and Yusuke Yamaya[1]

[1]Renewable Energy Research Center, National Institute of Advanced Industrial Science and Technology

SUMMARY

In order to investigate the performance of three-dimensional (3D) inversion of magnetotelluric (MT) data for geothermal exploration, where accurate numerical modeling is indispensable for coping with rough topography, we have utilized two inversion codes, FEMTIC and WSINV3DMT, for 3D inversion of MT data obtained in Okuaizu geothermal area, northern Japan. FEMTIC, a finite-element (FEM) inversion code, can incorporate either tetrahedral elements (Tetra) or deformed non-conforming hexahedral elements (DHexa) in the mesh, while WSINV3DMT, a finite-difference (FDM) inversion code, uses rectangular cells. We prepared the same subset of MT data (all components of the impedance and tipper at 16 frequencies from 58 stations) and set the same noise-floor for running Tetra, DHexa and WSINV3DMT inversions. As a result, all three inversions gave similar 3D models, indicating resistivity anomalies related to the cap rock and the geothermal reservoir in the area. However, the model by WSINV3DMT generated some irregular features; (1) several thin horizontal anomalies of high- and low-resistivities alternately appeared in shallow parts, which was not realistic, and (2) the conductive anomaly at depth of 3-5 km showed extremely low resistivity value. This suggests that the FEM inversion is more stable than FDM when we include the topography in the inversion.

Keywords: magnetotellurics, three-dimensional inversion, finite element, finite difference, topography, Okuaizu geothermal area

INTRODUCTION

Application of the magnetotelluric (MT) method for geothermal exploration has rapidly expanded worldwide since a decade ago. Particularly, three-dimensional (3D) inversion has become a routine task in the interpretation. It is because a few sophisticated 3D inversion codes, such as WSINV3DMT (Siripunvaraporn and Egbert, 2009) and ModEM (Kelbert et al., 2014), are public and help many geothermal engineers. These codes use the finite-difference method (FDM) for the forward modeling. However, it is well known that the numerical accuracy often decreases when we incorporate the topography in the FDM modeling due to the large resistivity contrast between the air and the underground.

3D MT inversion codes that use the finite-element method (FEM) for the forward modeling have been published since several years ago (e.g., Grayver, 2015; Usui, 2015; Kordy et al., 2016; Jahandari and Farquharson, 2017). The FEM can flexibly incorporate the topography variation in the mesh without reducing the numerical accuracy much.

The code, FEMTIC (Usui, 2015), became public domain in 2021. In this study, we ran the 3D inversion of the MT data obtained in Okuaizu geothermal area, northern Japan, using both FEMTIC and WSINV3DMT, and investigated the performance of the codes when we include the topography.

MT DATA

The Okuaizu geothermal area is located in a small caldera that was formed approximately 300,000 years ago (Mizugaki, 2000). All of geological formations surveyed by past geothermal drillings are volcanic origin in Neogene and Quaternary time, except intermittent sedimentary layers and shallow alluvium. A 30 MWe geothermal power plant has been in operation since 1995.

MT surveys were conducted over the Okuaizu geothermal area at two stages (Uchida et al., 2015). The first survey was conducted in 2000 and 2001 as a 2D survey along two long profiles (roughly NE-SW and NW-SE) crossing the central zone of the geothermal area. The second one was a 3D survey in 2010 concentrating in the central zone, with 30 MT stations covering roughly an area of 3.5 km x 3.5 km with an average station interval of 500 m. The MT data were obtained using Phoenix MTU-5A systems, and the remote reference station was deployed at about 200 km north from the survey area. In this study, we set an area of approximately 8 km north-south and 10 km east-west for the 3D interpretation, utilizing the data from 58 MT stations (Figure 1).

INVERSION PROCEDURE

We used two inversion codes, FEMTIC (Usui, 2015; Usui et al., 2017) and WSINV3DMT (Siripunvaraporn

and Egbert, 2009). FEMTIC, a finite-element modeling (FEM) code, can incorporate either tetrahedral elements or deformed non-conforming hexahedral elements in the 3D mesh, while WSINV3DMT, a finite-difference modeling (FDM) code, uses rectangular cells.
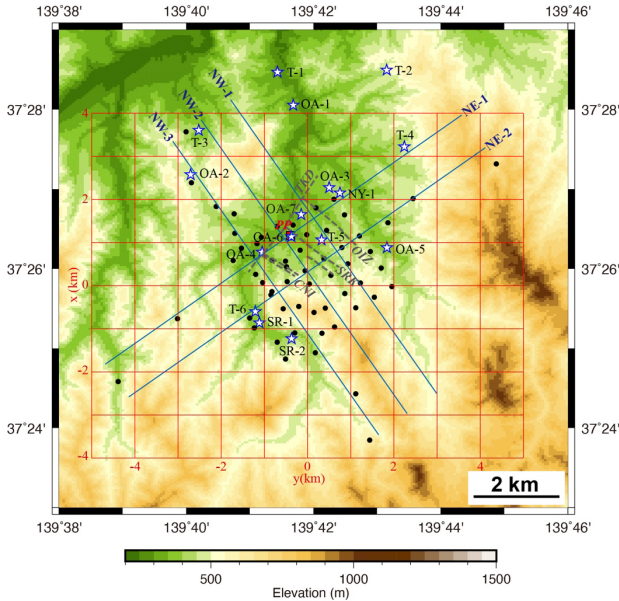
Fig. 1: Location of MT stations (black dots) on a topography contour map in the Okuaizu area. Stars are boreholes by past geothermal surveys and the red square with '*PP*' indicates the location of Yanaizu-Nishiyama geothermal power plant (main building). Grey dashed lines are estimated faults which the geothermal reservoir is associated with. Blue lines are profiles for showing cross-sections and red grids for showing plan views of the 3D model.

Figure 2 shows the mesh setting for the tetrahedral elements (Tetra) and deformed non-conforming hexahedral elements (DHexa) for the FEMTIC code, and rectangular cells for WSINV3DMT (WS3D). The size of the smallest element was less than 25 m for Tetra, while about 30 m horizontally and 25 m vertically for Dhexa near MT stations, and it gradually increased as we moved away from the stations (Fig. 2a, 2b). The size of rectangular cells near the earth surface was 150 m horizontally and 10 m vertically for the WS3D mesh (Fig. 2c). For Tetra, several elements were grouped into a block that was given the same resistivity in the inversion. The smallest block size was less than 40 m near MT stations, and it gradually increased as we moved away from the stations. For DHexa and WS3D, resistivity values of all elements (cells), except the air and sea water, were dealt as unknown parameters individually in the inversion.

The initial model was a homogeneous underground of 30 ohm-meters, which was close to the average value of observed apparent resistivities. Resistivity of the seawater was set as 0.33 ohm-meter. The air resistivity was 10^8 ohm-meters for FEMTIC and 10^7 ohm-meters for WS3D.
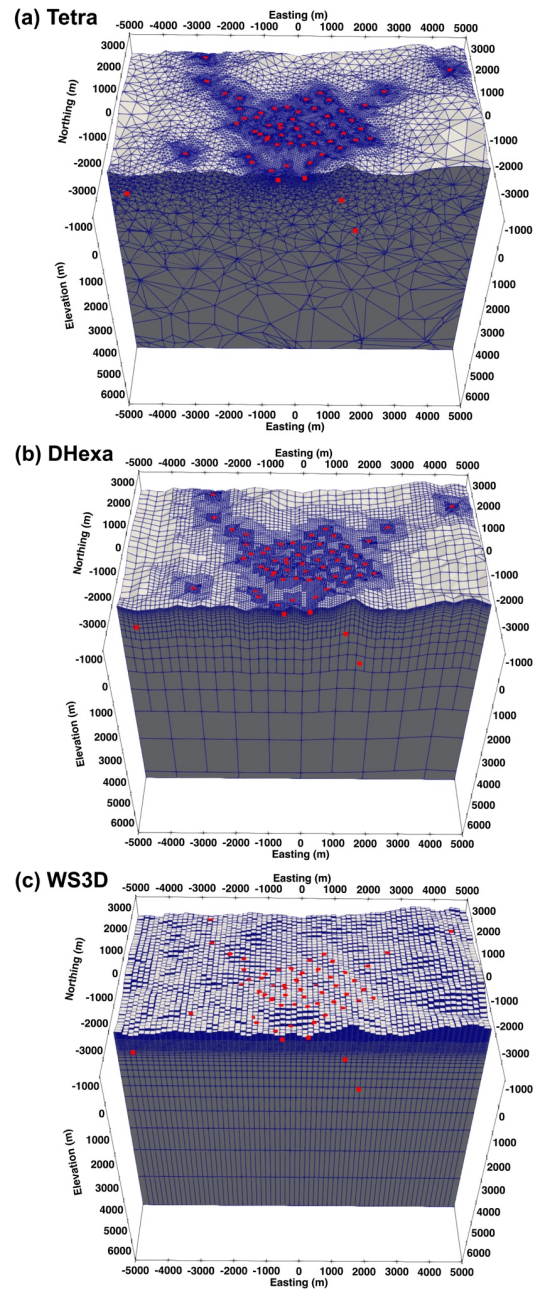
Fig. 2: Mesh setting for (a) tetrahedral (Tetra) elements and (b) deformed non-conforming hexahedral (DHexa) elements for the FEMTIC inversion, and (c) rectangular cells for WSINV3DMT (WS3D) inversion in the core zone of the mesh. Red dots indicate MT stations.

We used the same subset of MT data for all inversions; all components of the impedance and tipper at 16 frequencies (0.00275 – 97 Hz) at 58 stations. We set the same noise-floor for FEMTIC and WS3D; 3% for the off-diagonal components and 9% for the diagonal components of the impedance, and 0.008 for tipper. They were approximately 80% of median values of observation errors of all data used for the inversion. The data quality of this area was not so good at the low frequency band,

because the terminal station of a DC train system was located only some 20 km south, and noises by leak currents from the railway were dominant in the majority of the time-series segments (Uchida et al., 2015).

Galvanic distortion was included as unknowns in the FEMTIC inversion. Final RMS misfit achieved was 1.298, 1.420 and 1.691 for Tetra, DHexa and WS3D, respectively. Note that a target RMS misfit was set as 1.7 for the WS3D inversion in order to prevent the model become too rough.

INVERSION RESULTS

Figure 3 compares elevation-slice sections of the 3D models by Tetra, DHexa and WS3D inversions. Resistivity distribution of Tetra and DHexa is similar from the surface to an elevation of -3 km, but the location of low-resistivity anomaly is different at the -5 km elevation. Resistivity distribution of the WS3D model is generally similar to those of FEMTIC but slightly different for all five sections. Resistivity of the low-resistivity anomaly at -3 km and -5 km elevation is very low in the WS3D model.

Figures 4 and 5 compare resistivity distribution along NE-SW and NW-SE cross-sections. In the central zone, resistivity is generally low from the surface to approximately -1 km elevation. It corresponds with a clay-alteration zone and works as a cap rock of the geothermal reservoir. Below it is a relatively higher resistivity zone that corresponds to the high-temperature reservoir zone. A low-resistivity columnar anomaly of 1 - 2 km diameter and depth extension from -1 to -6 km (or more) elevation exists beneath the location of the power plant. The shape of this columnar anomaly differs between the three models. We can observe that several thin horizontal anomalies of high- and low-resistivities alternately appeared in shallow parts in the WS3D model, which is not realistic (Figures 4c and 5c).

Figure 6 is a bird-eye view of the Tetra model, showing low-resistivity elements of less than 5 ohm-meters. This figure clearly shows the combination of low-resistivity cap rock that includes low-temperature clay minerals (such as smectite) and higher-resistivity reservoir zone that includes high-temperature clay minerals (such as chlorite). In addition, a deep conductor, which may be related to the heat source or high-temperature fluid for the geothermal system, is obtained.

CONCLUSION

We applied two inversion codes, FEMTIC and WSINV3DMT, for the 3D inversion of MT data obtained in Okuaizu geothermal area, incorporating the topography. Both codes successfully generated similar 3D models that indicated good agreement with the geothermal structure. However, there are differences between the three models (Tetra, DHexa and WS3D) and further study is necessary to understand the reliability of the models.

REFENRECES

Grayver, A.V. (2015) Parallel three-dimensional magnetotelluric inversion using adaptive finite-element method. Part I: theory and synthetic study. *Geophys. J. Int.*, **202**, 584-603, doi:10.1093/gji/ggv165.

Jahandari, H., Farquharson, C.G. (2017) 3-D minimum-structure inversion of magnetotelluric data using the finite-element method and tetrahedral grids. *Geophys. J. Int.*, **211**, 1189-1205. doi:10.1093/gji/ggx358.

Kelbert, A., Meqbel, N., Egbert, G.D., Tandon, K. (2014) ModEM: A modular system for inversion of electromagnetic geophysical data. *Computers & Geosciences*, **66**, 40–53. doi:10.1016/j.cageo.2014.01.010.

Kordy, M., Wannamaker, P., Maris, V., Cherkaev, E., Hill, G. (2016) 3-D magnetotelluric inversion including topography using deformed hexahedral edge finite elements and direct solvers parallelized on SMP computers – Part I: forward problem and parameter Jacobians. *Geophys. J. Int.*, **204**, 74–93. doi:10.1093/gji/ggv410.

Mizugaki, K. (2000) Geologic structure and volcanic history of the Yanaizu-Nishiyama (Okuaizu) geothermal field, Northeast Japan, *Geothermics*, **29**, 233-256.

Siripunvaraporn, W., Egbert, G. (2009) WSINV3DMT: Vertical magnetic field transfer function inversion and parallel implementation. *Physics of the Earth and Planetary Interiors*, **173**, 317-329. doi:10.1016/j.pepi.2009.01.013.

Uchida, T., Takakura, S., Ueda, T., Sato, T., Abe, Y. (2015) Three-Dimensional Resistivity Structure of the Yanaizu-Nishiyama Geothermal Reservoir, Northern Japan. *Proceedings of World Geothermal Congress 2015*, Melbourne, Australia, 7p.

Usui, Y. (2015) 3-D inversion of magnetotelluric data using unstructured tetrahedral elements: applicability to data affected by topography. *Geophys. J. Int.*, **202**, 828-849. doi:10.1093/gji/ggv186.

Usui, Y., Ogawa, Y., Aizawa, K., Kanda, W., Hashimoto, T., Koyama, T., Yamaya, Y., Kagiyama, T. (2017) Three-dimensional resistivity structure of Asama Volcano revealed by data-space magnetotelluric inversion using unstructured tetrahedral elements. *Geophys. J. Int.*, **208**, 1359-1372. doi:10.1093/gji/ggw459.
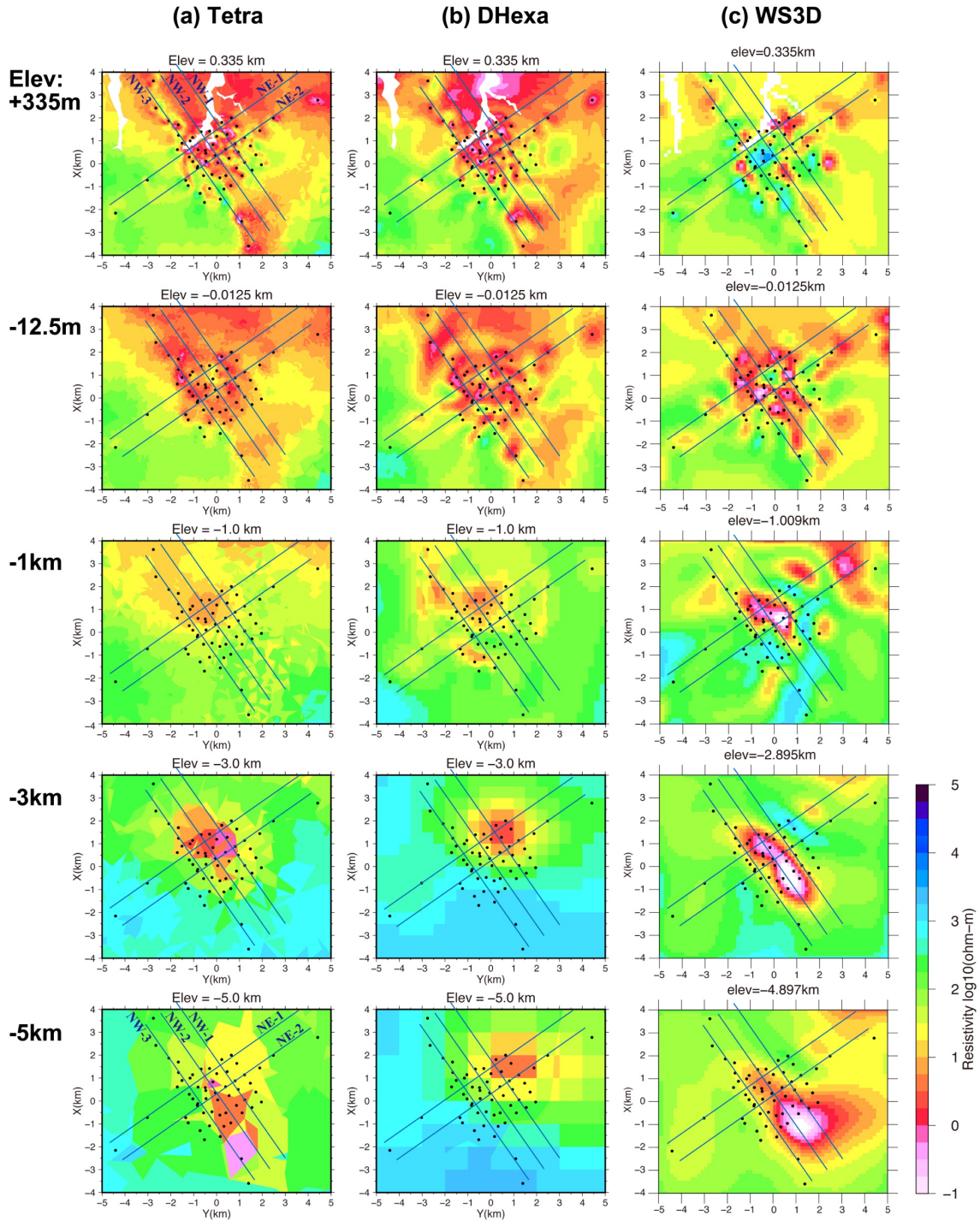
Fig. 3: Plan views of the 3D resistivity models at five elevations of 0.335 km, -0.0125 km, -1 km, -3 km and -5 km for Tetra, DHexa and WS3D inversions, respectively. Black dots are MT stations. Solid lines indicate the profiles shown in Figures 4 and 5.
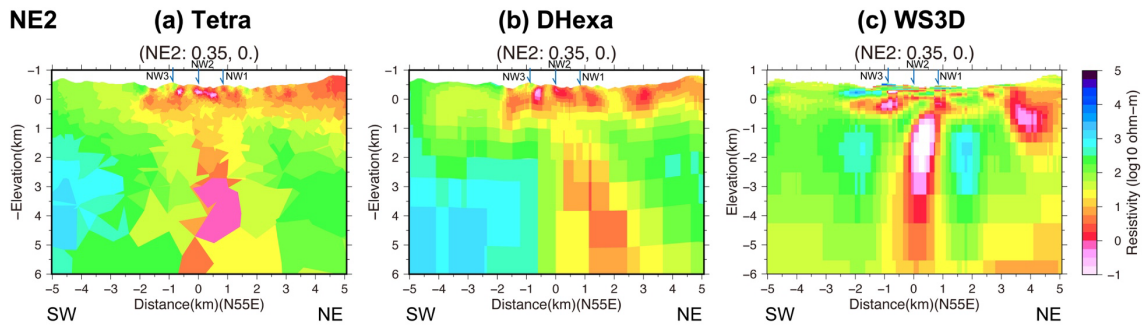
Fig. 4: Resistivity distribution along northeast-southwest cross-section, NE2, for (a) Tetra, (b) DHexa and (c) WS3D inversions. The 0 km distance corresponds to the position of x=0.35 km and y=0 km.
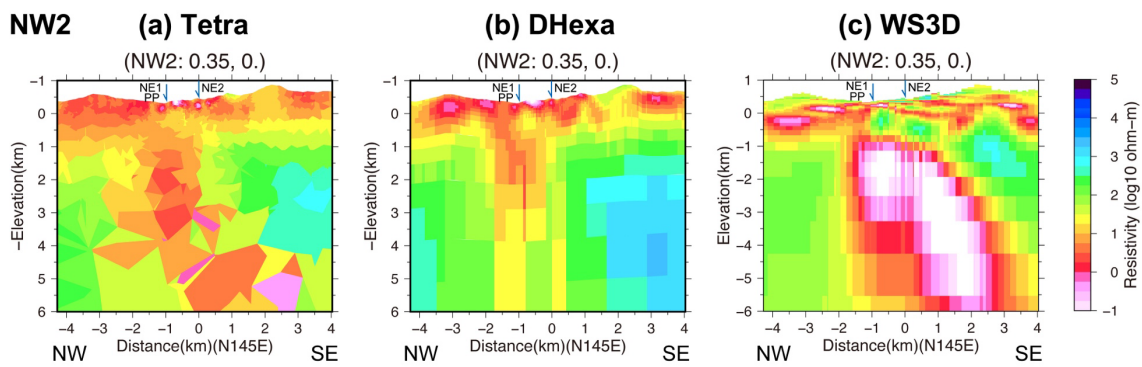
Fig. 5: Resistivity distribution along northwest-southeast cross-section, NW2, (a) Tetra, (b) DHexa and (c) WS3D inversions. The 0 km distance corresponds to the position of x=0.35 km and y=0 km.
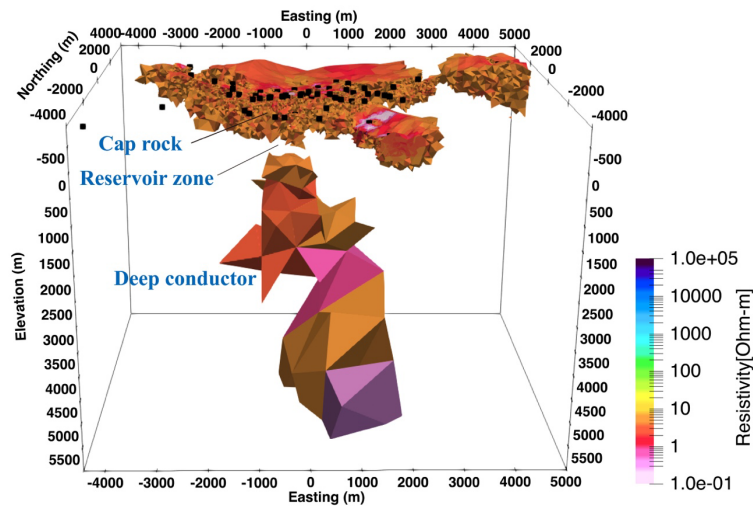
Fig. 6: A bird-eye view (looking from south) of the 3D model by the Tetra inversion, showing elements whose resistivity is lower than 5 ohm-meters.